A unified model for jet, heavy and passive dispersion including droplet rainout and re-evaporation

by

H.W.M. Witlox and A. Holt
Det Norske Veritas, London, UK

Abstract

The Unified Dispersion Model (UDM) models the dispersion following a ground-level or elevated two-phase unpressurised or pressurised release. It allows for continuous, instantaneous, constant finite-duration, and general time-varying releases. It includes a unified model for jet, heavy and passive two-phase dispersion including possible droplet rainout, pool spreading and re-evaporation. It calculates the phase distribution and cloud temperature using either a non-equilibrium thermodynamics model, a non-reactive equilibrium model, or an equilibrium model specific for HF (including effects of polymerisation).

As part of the current work each of the modules in the UDM (passive, jet, and heavy dispersion; non-equilibrium, equilibrium and HF thermodynamics; steady, instantaneous or finite-duration releases; pool spreading/evaporation on land or water) has been investigated. The fundamental underlying physics has been considered in conjunction with a literature review, comparison against wind-tunnel experiments, verification of the numerical solution against analytical solutions (where possible) and sensitivity analyses. In addition the model has been compared against predictions by third-party models such as the HGSYSTEM dispersion model HEGADAS and the pool model GASP.

As a result of this work the tuning present in the original UDM model has largely been eliminated, and model coefficients are obtained directly from established data in the literature which are largely based on wind-tunnel experiments. The latest UDM version implemented in the DNV software application PHAST 6.0 represents a significant revision and extension to all parts of the model. This paper includes an overview of the new model and a summary of the module verification and validation.

The paper also includes a description of the validation of the overall UDM model against large-scale field experiments. The validation set of experiments includes both continuous and instantaneous releases. These experiments address complex phenomena such as aerosol discharges and HF thermodynamics, in addition to relatively simplistic releases. A subset of these experiments include those evaluated as part of the EEC programme SMEDIS (**S**cientific **M**odel **E**valuation of **D**ense Gas D**is**persion Models).

1. Introduction

This paper describes the new version of the Unified Dispersion Model (UDM) implemented into the DNV software package PHAST 6.0. The original version of UDM was developed by Woodward and Cook[1,2] as new technology in the early nineties. The new UDM 6.0 version represents a significant revision and extension to all parts of the model. This has been carried out in conjunction with a detailed literature review, verification and validation of the model.

The UDM models the dispersion following a ground-level or elevated two-phase pressurised release. It effectively consists of the following linked modules (see Figure 1 and Figure 8):

- jet dispersion
- droplet evaporation and rainout, touchdown
- pool spread and vaporisation
- heavy gas dispersion
- passive dispersion

A single form of concentration profile is used to cover all stages of a release. This allows for anything from a sharp-edged profile in the initial stages of a jet release through to the diffuse Gaussian profile that would be expected in the final passive stage of spreading.

The UDM includes the effects of droplet vaporisation using a non-equilibrium model (see Figure 8). Rainout produces a pool which spreads and vaporises. Vapour is added back into the plume and allowance is made for this additional vapour flow to vary with time. In addition to the non-equilibrium model, UDM also allows for an equilibrium model and an equilibrium model specific for HF (including effects of polymerisation).

The UDM allows for vertical variation in ambient wind speed, temperature and pressure. Another feature of the UDM is possible plume lift-off, where a grounded cloud becomes buoyant and rises into the air. Rising clouds may be constrained to the mixing layer if it is reached.

The UDM allows for continuous, instantaneous, constant finite-duration, and general time-varying releases.

For the original UDM Cook and Woodward adopted a tuning process, where the tuning coefficients were obtained by the comparison of UDM results against a relatively large set of 'tuning' experiments. This type of tuning has largely been eliminated as part of the current work. The model coefficients have now been obtained directly from established data in the literature (based on wind-tunnel experiments), rather than doing UDM simulations and fitting the UDM results to the experimental data.

Sections 2, 3, and 4 of this paper include a description of the theory, verification and module validation of the UDM dispersion model, the UDM thermodynamics, and the UDM pool spreading/evaporation model. Section 5 summarises the validation of the overall UDM model against large-scale field experiments. In Section 6 the major conclusions are summarised. The reader is referred to the UDM Technical Reference Manual[3] for details not included in the present paper.

2. Dispersion model

2.1   *Concentration profile and cloud geometry*

Figure 1 shows the movement of the cloud in the downwind direction. The Cartesian co-ordinates x, y, z correspond to the downwind,   cross-wind (lateral horizontal) and vertical directions, respectively;   x=0 corresponds to the point of release, y = 0 to the plume centre-line and z = 0 to ground-level. Furthermore s is the arc length measured along the plume centre, θ the angle between the plume centre-line and the horizontal, and ζ the distance from the plume centre-line.

The concentration c is given by a similarity profile c = c(x,y,ζ) as suggested by Webber et al.[4]

$$c(x,y,\zeta)=c_o(x)F_v(\zeta)F_h(y),\ with\ F_v(\zeta)=\exp\left\{-\left|\frac{\zeta}{R_z}\right|^n\right\},\ F_h(y)=\exp\left\{-\left|\frac{y}{R_y}\right|^m\right\},\ (continuous) \tag{1}$$

$$c(x,y,\zeta;t)=c_o(t)F_v(\zeta)F_h(r),\ with\ horizontal\ radius\ \ r=\sqrt{(x-x_{cld})^2+y^2}\ ,\ \ (instantaneous) \tag{2}$$

In case of steady-state dispersion, Equation (1) describes exponential decay of the concentration in y and ζ in terms of the cross-wind and vertical dispersion coefficients $R_y(x)$, $R_z(x)$. Empirical correlations are adopted for the exponents m, n such that the near-field sharp-edged profile (large value for m) develops into a Gaussian profile in the far field (m=2). As shown in Figure 1a, the plume cross-section is a circle (radius $R_y=R_z$) during elevated jet dispersion, a truncated circle during touching down, and a semi-ellipse after touching down. The area of this plume cross-section, $A_{cld}(x)$, is obtained by integration of $F_v(\zeta)F_h(y)$ over y,ζ. As in many other dispersion models, the cloud is also characterised by an equivalent 'effective cloud' [rectangular cross-section with area A_{cld}, effective half-width $W_{eff}(x)$, and effective height $H_{eff}(x)(1+h_d)$ with h_d=0 for grounded plume and

----

h_d=1 for elevated plume] with centroid cloud speed u_{cld}, and equivalent top-hat concentration equal to the centre-line concentration $c_o(x)$.

In the case of instantaneous dispersion, the cloud moves in the downwind direction with cloud centre at time t denoted by $x=x_{cld}(t)$, $y=0$, $z=z_{cld}(t)$. Equation (2) describes exponential decay of the concentration in x, y, ζ=z-z_{cld} in terms of the horizontal and vertical dispersion coefficients $R_y(t)$, $R_z(t)$, with downwind spreading assumed to be equal to cross-wind spreading ($R_x=R_y$). As shown in Figure 1b, the cloud is a sphere (radius $R_y=R_z$) during elevated jet dispersion, a truncated sphere during touching down, and a semi-ellipsoid after touching down. The volume of this cloud, V_{cld}, is determined by integration $F_v(\zeta)F_h(r)$ over x, y, ζ. The cloud is also characterised by an equivalent 'effective cloud' [cylindrical shape with volume V_{cld}, effective horizontal radius W_{eff}, and effective height $H_{eff}(1+h_d)$] with centroid cloud speed u_{cld}, and equivalent top-hat concentration equal to the centre-line concentration $c_o(t)$.

2.2   Dispersion variables and equations

The model evaluates the plume variables as a function of downwind distance. The plume variables are given in the table below {$u_a(z_c)$ = wind speed at centroid height z_c, $[u_x,u_z]=u_{cld}[\cos \theta, \sin \theta]$ = cloud speed }

plume variable	symbol	unit (continuous)	unit (instantaneous)
mass of the cloud	m_{cld}	kg/s	kg
excess downwind momentum	$I_{x2} = m_{cld}[u_x - u_a(z_c)]$	kg m/s^2	kg m/s
vertical momentum	$I_z = m_{cld} u_z$	kg m/s^2	kg m/s
downwind position	x_{cld}	m	m
vertical position	z_{cld}	m	m
heat conduction from substrate	q_{gnd}	J/s	J
water evaporated from substrate	m_{wv}^{gnd}	kg/s	kg
cross-wind dispersion coefficient	R_y	m	m

After initialisation at the point of release, these variables are determined by solving a set of ordinary differential equations forward in the downwind direction (continuous) or time (instantaneous). These equations express conservation of mass (air entrainment and water added from substrate), conservation of momentum, relation between cloud speed and cloud position, a heat-transfer relation, a water-vapour transfer relation, and a cross-wind spreading equation. These equations are described below (see the UDM Technical Reference Manual[3] for full details).

- *Conservation of total cloud mass*

$$\frac{d\,m_{cld}}{ds} = E_{tot} + \frac{dm_{wv}^{gnd}}{ds} \qquad , \quad \text{(continuous)} \tag{3}$$

$$\frac{d\,m_{cld}}{dt} = E_{tot} + \frac{dm_{wv}^{gnd}}{dt} \qquad , \text{(instantaneous)} \tag{4}$$

The above equation expresses the change in cloud mass as a result of entrainment of air into the cloud and (in case of dispersion over water) water-vapour transfer from the substrate. The total air entrainment is E_{tot} (kg/m/s for continuous, and kg/s for instantaneous dispersion).

Air entrainment into a plume may be caused by a range of mechanism (see Figure 2). Jet entrainment and crosswind entrainment are dominant in the near field after a high-pressure continuous release. During the jet dispersion phase, the centreline velocity decays until either the heavy gas or the passive dispersion mechanisms become dominant. For a low-energy release, the jet dispersion mode may never be dominant. A transition is made to passive dispersion if the cloud density is sufficiently close to the ambient density (for heavy gas dispersion the Richardson number must be sufficiently small), the cloud speed is sufficiently close to the ambient speed and the contribution of non-passive entrainment is sufficiently small. The entrainment contributions are calculated as follows:

----

1. Jet entrainment E_{jet} is caused by turbulence resulting from the difference between the jet speed and the ambient wind speed:

$$E_{jet} = e_{jet} \; P_{above} \; \rho_a \; |u_{cld} - u_a \cos\theta| \quad \text{in} \quad \text{kg/m/s} \quad \text{(continuous)} \qquad (\,5\,)$$

$$E_{jet} = e_{jet} \; S_{above} \; \rho_a \; |u_{cld} - u_a \cos\theta| \quad \text{in} \quad \text{kg/s} \quad \text{(instantaneous)} \qquad (\,6\,)$$

where ρ_a is the ambient density, P_{above} the cross-wind perimeter (m) of the continuous plume above the ground (m), and S_{above} the instantaneous cloud surface area above the ground (m^2). Equation (5) for continuous dispersion is the Morton-Taylor-Turner formulation[5], and Equation (6) is a generalised version for instantaneous dispersion. Assuming a jet of uniform density (top-hat profile), Ricou and Spalding[6] determined from experiments $\alpha_1 = 2\pi^{0.5}e_{jet} = \pi^{0.5}\tan(\beta_\infty) = 0.282$, where $\beta_\infty = 9.1^\circ$ is the empirical value of the asymptotic half-angle of the jet. Ratios between 1.5 and 2.0 have found to be quoted in the literature for conversion between top-hat (averaged) concentrations and maximum concentrations. Since the value of the observed maximum concentrations was approximately 70% larger, we adopt $\alpha_1 = 0.282/1.7 = 0.17$.

2. Cross-wind entrainment E_{cross} in response to the deflection of the plume by the wind:

$$E_{cross} = \alpha_2 \rho_a P_{above} |u_a \sin\theta| \quad \text{in kg/m/s} \quad \text{(continuous)} \qquad (\,7\,)$$

$$E_{cross} = \alpha_2 \rho_a S_{above} |u_a \sin\theta| \quad \text{in kg/s} \quad \text{(instantaneous)} \qquad (\,8\,)$$

Equation (7) for continuous dispersion is from Morton et al.[5], and Equation (8) is a generalised version for instantaneous dispersion. The value for α_2 adopted by Briggs[7] is 0.6 for a top-hat profile. Again the value of the maximum concentrations is assumed to be 70% larger, and therefore we adopt $\alpha_2 = 0.6/1.7 = 0.35$.

3. Passive entrainment is caused by ambient turbulence; it is present both in the near-field (E_{pas}^{nf}) and the far-field (E_{pas}^{ff}). For continuous elevated dispersion, the near-field passive entrainment formulation is taken from McFarlane[11] derived from experiments by Disselhorst[8], while for instantaneous dispersion a generalised version is adopted. The far-field passive entrainment is derived from empirical correlations $\sigma_{ya}(x)$ and $\sigma_{za}(x)$ for the Gaussian cross-wind and vertical dispersion coefficients as a function of x.

4. Heavy-gas entrainment E_{hvy} is included for a grounded heavy-gas plume:

$$E_{hvy} = \left[\frac{W_{gnd}}{R_y}\right] u_{top}(2W_{eff}) \; \rho_a \,, \qquad u_{top} = \frac{\kappa \, u_*}{\Phi(\,Ri_*\,)} \,, \qquad \text{(continuous)} \qquad (\,9\,)$$

$$E_{hvy} = \left[\frac{W_{gnd}}{R_y}\right] \{u_{side} A_{side} + u_{top} A_{top}\} \, \rho_a \,, \qquad u_{side} = \gamma \, \frac{dW_{eff}}{dt} \,, \quad \text{(instantaneous)} \qquad (\,10\,)$$

Here u_{top} is the top-surface entrainment velocity, $\kappa = 0.4$ the Von Karman constant, u_* the friction velocity and $\Phi(Ri_*)$ the entrainment function of the Richardson number Ri_*. For instantaneous dispersion, u_{side} is the side entrainment velocity, γ the side entrainment coefficient, A_{side} the side area and A_{top} the top area [for grounded plume, $A_{side} = 2\pi W_{eff}H_{eff}$, and $A_{top} = \pi W_{eff}^2$]. The entrainment function Φ is taken from Havens and Spicer[9] for $Ri_* < 0$ and from Britter[10] for $Ri_* > 0$. This ensures the best fit for the top-entrainment velocity against a wide range of experimental data. Finally W_{gnd} is the cross-wind radius of the part of the cloud touching the ground. Thus the term W_{gnd}/R_y in Equations (9),(10) ensures that heavy-gas entrainment is gradually phased in

----

during touching down, i.e. from the elevated plume ($W_{gnd}/R_y=0$) to the ground-level plume ($W_{gnd}/R_y=1$).

- *Conservation of excess horizontal and vertical component of momentum*

  The adopted momentum equations (vector notation) are as follows for continuous dispersion [cloud area $A_{cld} = m_{cld} / (\rho_{cld}u_{cld})$, where ρ_{cld} is the cloud density] or instantaneous dispersion [cloud volume $V_{cld} = m_{cld} / \rho_{cld}$],

$$\begin{bmatrix} \dfrac{dI_{x2}}{ds} \\ \dfrac{dI_z}{ds} \end{bmatrix} = F_{impact}^{ground} \begin{bmatrix} -\sin\theta \\ 0 \\ \cos\theta \end{bmatrix} + F_{drag}^{ground} \begin{bmatrix} 1 \\ 0 \end{bmatrix} + A_{cld}(\rho_{cld} - \rho_a)g \begin{bmatrix} 0 \\ -1 \end{bmatrix}, \quad \text{(continuous)} \tag{11}$$

$$\begin{bmatrix} \dfrac{dI_{x2}}{dt} \\ \dfrac{dI_z}{dt} \end{bmatrix} = F_{impact}^{ground} \begin{bmatrix} -\sin\theta \\ 0 \\ \cos\theta \end{bmatrix} + F_{drag}^{ground} \begin{bmatrix} 1 \\ 0 \end{bmatrix} + V_{cld}(\rho_{cld} - \rho_a)g \begin{bmatrix} 0 \\ -1 \end{bmatrix}, \quad \text{(instantaneous)} \tag{12}$$

The terms in the right-hand side represent forces on the plume. They are respectively:

- the ground impact force F_{impact}^{ground} (N/m or N) resulting from plume collision with the ground. This force is perpendicular to the plume centre line, and is added during touching down only.
- the horizontal ground drag force F_{drag}^{ground} (N/m or N). This force is added after onset of touchdown only.
- the vertical buoyancy force (N/m or N). This force is proportional to the gravitational acceleration g (= 9.81 m²/s) and the density difference between the plume and the air.

The vertical momentum equation is not used when the cloud is grounded or capped at the mixing layer (constant plume height). The formulas for the ground drag and ground impact forces are partly taken from McFarlane[11] for continuous dispersion, and have been generalised for application to instantaneous dispersion.

- *Horizontal and vertical position:*

$$\frac{dx_{cld}}{ds} = \cos\theta, \qquad \frac{dz_{cld}}{ds} = \sin\theta, \quad \text{(continuous)} \tag{13}$$

$$\frac{dx_{cld}}{dt} = u_x = u_{cld}\cos\theta, \qquad \frac{dz_{cld}}{dt} = u_z = u_{cld}\sin\theta, \quad \text{(instantaneous)} \tag{14}$$

- *Rate of heat convection from the substrate*

  The heat convection from the substrate to the cloud is described by the following differential equation,

$$\frac{d\,q_{gnd}}{ds} = Q_{gnd}\,[2W_{gnd}], \quad in\ W/m \ \text{(continuous)} \tag{15}$$

$$\frac{d\,q_{gnd}}{dt} = Q_{gnd}\,S_{gnd}, \quad in\ W \ \text{(instantaneous)} \tag{16}$$

In case of continuous releases, dq_{gnd}/ds (J/m/s) is the heat transferred from the substrate per second and per unit of downwind direction and W_{gnd} is the half-width of the cloud in contact with the substrate [see Figure 1a]. In case of instantaneous releases q_{gnd} is the total heat (J) transferred from the substrate to the cloud and S_{gnd} is the area of the cloud in contact with the substrate [see Figure 1b]. The heat conduction flux Q_{gnd} (W/m²) transferred from the substrate (temperature T_{gnd}) to the cloud (vapour temperature T_{vap}) is given by

$$
\begin{aligned}
Q_{gnd} &= \max\left\{ Q_{gnd}{}^n, Q_{gnd}{}^f \right\}, & T_{gnd} &> T_{vap} \\
&= Q_{gnd}{}^f, & T_{gnd} &\leq T_{vap}
\end{aligned}
\qquad (17)
$$

where $Q_{gnd}{}^n$ and $Q_{gnd}{}^f$ are the natural and forced convection flux from the substrate to the vapour cloud (W/m²) derived from expressions by McAdams (1954)[12] and Holman (1981)[13], respectively.

- *Water-vapour transfer from the substrate*

  Water vapour can be transferred from a water surface into the cloud when the vapour temperature of the cloud is less than that of the water surface. This has been included in the Unified Dispersion Model following the approach of the Colenbrander and Puttock described by Witlox[14] which relates the rate of water vapour pick-up to the rate of heat convection from the water surface:

$$
\frac{dm_{wv}^{gnd}}{ds} = \frac{5\left[P_v{}^w(T_{gnd}) - P_v{}^w(T_{vap}) \right] \dfrac{dq_{gnd}}{ds}}{C_p{}^{cld} T_{gnd} P_a}, \quad T_{gnd} > T_{vap} \text{ (continuous)}
\qquad (18)
$$

$$
\frac{dm_{wv}^{gnd}}{dt} = \frac{5\left[P_v{}^w(T_{gnd}) - P_v{}^w(T_{vap}) \right] \dfrac{dq_{gnd}}{dt}}{C_p{}^{cld} T_{gnd} P_a}, \quad T_{gnd} > T_{vap} \text{ (instantaneous)}
\qquad (19)
$$

  where $P_v{}^w$ is the saturated vapour pressure of water. If $T_{gnd} < T_{vap}$ or $T_{gnd} < 0°C$ (substrate is ice) or if the cloud is passing over dry ground, $dm_{wv}{}^{gnd}/ds = 0$ (continuous) or $dm_{wv}{}^{gnd}/dt = 0$ (instantaneous).

- *Crosswind spreading*

  In general cross-wind spreading consists of the following three subsequent phases (see Figure 2).

  1. <u>Jet spreading.</u> The cloud is assumed to remain circular until the passive transition or until the spread rate reduces to the heavy-gas spread rate (the latter can only occur after touchdown), i.e.

$$
R_y = R_z
$$

  2. <u>Heavy-gas spreading.</u> The heavy spread rate is applied until the passive transition. For instantaneous dispersion it is given by

$$
\frac{dR_y}{dt} = \frac{C_E}{C_m} \sqrt{\frac{g\left\{ \max\left[0, \rho_{cld} - \rho_a(z = z_c)\right] \right\} H_{eff}(1 + h_d)}{\rho_{cld}}}, \quad C_m = \left[\Gamma\left(1 + \frac{2}{m}\right) \right]^{1/2}
$$

  and for continuous dispersion by

$$
\frac{dR_y}{dx} = \frac{C_E}{u_x C_m} \sqrt{\frac{g\left\{ \max\left[0, \rho_{cld} - \rho_a(z = z_c)\right] \right\} H_{eff}(1 + h_d)}{\rho_{cld}}}, \quad C_m = \Gamma\left[1 + \frac{1}{m}\right]
$$

----

where $C_E = 1.15$ is the cross-wind spreading parameter from experiments by Van Ulden[15], and Γ is the gamma function. Note that $C_m = W_{eff}/R_y$.

3. <u>Passive spreading</u>. After the passive transition the passive spread rate is applied

$$\frac{dR_y}{dx} = 2^{0.5} \frac{d\sigma_{ya}}{dx}, \text{ (continuous)}$$

$$\frac{dR_y}{dt} = u_x 2^{0.5} \frac{d\sigma_{ya}}{dx}, \text{ (instantaneous releases)}$$

where $\sigma_{ya}(x)$ is the ambient passive cross-wind dispersion coefficient; σ_{ya} increases with averaging time as a result of wind meander.

2.3   Module verification and validation

The UDM Technical Reference Manual[3] includes a detailed description of the UDM verification for the near-field elevated (jet) dispersion, the ground-level heavy-gas dispersion and the far-field passive dispersion. This verification can be summarised as follows.

1. <u>Jet and near-field passive dispersion.</u> For an elevated horizontal continuous jet (of air), the UDM numerical results are shown to be identical to the results obtained by an analytical solution. Very good agreement has been obtained against both the Pratte and Baines correlation[16] (no ambient turbulence, i.e. no near-field passive dispersion) and the Briggs correlation[7] (including ambient turbulence, i.e. including near-field passive dispersion); see Figure 3 for example results.

A sensitivity analysis has been carried out for a given base-case with parameter variations to the release height, release speed, release angle and transition criterion.

2. <u>Heavy-gas dispersion</u>. The UDM numerical results are shown to be in identical agreement against an analytical solution for a 2-D isothermal ground-level plume. The UDM has been validated against the set of three 2-D wind-tunnel experiments of McQuaid[17] (steady-state ground-level dispersion of CO_2). Good agreement was obtained for all experiments. Figure 4 includes the results for McQuaid experiment 3 for three types of UDM simulations, i.e.

   (i) $E_{tot} = E_{hvy}$ [inclusion of heavy entrainment only; too conservative assumption]
   (ii) $E_{tot} = E_{hvy}+E_{jet}$ [sum of heavy and 'jet' entrainment, with 'jet' entrainment resulting from difference between cloud and (lower) ambient speed at point of release]
   (iii) $E_{tot} = \max(E_{hvy},E_{jet})$ [this may be more appropriate than the above assumption since the 'heavy' and 'jet' entrainment mechanisms are not independent; this 'conservative' assumption is adopted for the final UDM model]

The new formulation has also been validated against the HTAG[18] experiments 139 and 140 (isothermal ground-level dispersion of **H**eavier **T**han **A**ir **G**as) and further verified against HGSYSTEM model results. Figure 5 includes the following results for experiment 140:

   (i) UDM run [with imposed HGSYSTEM wind-speed profile and concentration exponent n]
   (ii) HEGADAS run adopting standard passive dispersion coefficient σ_{ya} without inclusion of turbulence collapse of heavy-gas spreading [in line with UDM assumptions]
   (iii) HEGADAS run adopting experimentally observed σ_{ya} without collapse of gravity spreading
   (iv) HEGADAS run adopting experimentally observed σ_{ya} with collapse of gravity spreading

By comparing the results for (i) and (ii), it is concluded that UDM and HEGADAS predictions are in close agreement, if similar assumptions are adopted. This is an important verification of the correct implementation of the model. From the figure it is also inferred, that future implementation into the

----

UDM of collapse of gravity spreading may be desirable. Note however that this phenonmenon is important for a subset of heavy-gas dispersion problems only.

3. Far-field passive dispersion. For purely (far-field) passive continuous dispersion, the UDM numerical results are shown to be in close agreement with the vertical and crosswind dispersion coefficients and concentrations obtained from the commonly adopted analytical Gaussian passive dispersion formula. The same agreement has been obtained for the case of purely (far-field) passive instantaneous dispersion, while assuming along-wind spreading equal to cross-wind spreading in the analytical profile.

    A sensitivity analysis has been carried out for a base-case with parameter variations to the release height, averaging time, surface roughness length, stability class, release rate and wind speed.

2.4   Finite-duration releases

To model finite-duration releases with a uniform release rate, the UDM allows for the quasi-instantaneous (QI) model or the finite-duration correction (FDC) model.

The QI model models the initial phase as a continuous source (neglect of downwind gravity spreading and downwind diffusion). When the cloud width becomes 'large' with respect to the cloud length, the cloud is replaced by an 'equivalent' circular cloud, and the subsequent phase is modelled as an 'instantaneous' circular cloud. The disadvantage of the QI model is the abrupt transition (sometimes resulting in severe discontinuities, e.g. erroneous significant increase in maximum concentration). The QI model can be applied with or without the 'duration adjustment', where the duration adjustment applies the effect of averaging time because of time-dependency of the concentrations (for averaging times larger than release duration). The current duration adjustment over-estimates this effect downwind of the QI transition.

The FDC model is based on the HGSYSTEM formulation derived from that adopted in the SLAB dispersion model[19,20]. It has a better scientific basis and is derived from an analytical solution of the Gaussian plume passive-dispersion equations. It takes the effects of downwind diffusion gradually into account including effects of both turbulent spread and vertical wind shear. A limitation of this model is however that it is strictly speaking only applicable to ground-level non-pressurised releases without significant rainout. Moreover it produces predictions of the maximum (centre-line ground-level) concentrations only. The finite-duration correction includes the effect of averaging time because of time-dependency of the concentrations. The FDC module has been verified against the HGSYSTEM/SLAB steady-state results, and shown to lead to finite-duration corrections virtually identical to the latter programs.

3. Thermodynamics model

UDM invokes the thermodynamics module while solving the dispersion equations in the downwind direction. The module describes the mixing of the released component with moist air, and may take into account water-vapour and heat transfer from the substrate to the cloud. The module calculates the phase distribution [component (vapour, liquid), water (vapour, liquid, ice)], vapour and liquid cloud temperature, and cloud density. Thus separate water (liquid or ice) and component (liquid) aerosols may form.

The liquid component in the aerosol is considered to consist of spherical droplets and additional droplet equations may be solved to determine the droplet trajectories, droplet mass and droplet temperature. Rainout of the liquid component occurs if the droplet size is sufficiently large.

The UDM includes the following types of thermodynamic models:

1. Equilibrium model (no reactions). Thermal equilibrium is assumed, which implies that the same temperature is adopted for all compounds in the cloud (vapour and liquid). The equilibrium model determines the phase distribution and the mixture temperature. It is based on a simplified version of the multi-compound algorithm developed by Witlox for use in HGSYSTEM[21].

    The equilibrium model is tested for mixing of propane with moist air at 20C. Ambient humidity, propane liquid fraction, propane temperature have been varied. The cooling effect because of component evaporation and the heating effect because of water condensation is shown. The UDM equilibrium-

----

model predictions are shown in Figure 6 to be very close with HEGADAS predictions for the case of mixing of propane vapour/liquid (at –43/42C) with 0%/100% humid air.

2. Equilibrium model (HF). The same temperature is adopted for all compounds in the cloud (vapour and liquid). The model includes the effect of HF polymerisation and fog formation.

    The HF thermodynamics model is based on the HGSYSTEM thermodynamics model[22]. Therefore the UDM thermodynamic predictions are compared against those of HGSYSTEM, and predictions are shown to be consistent. This also implies that good agreement is obtained against Schotte's experiment[23] as is shown by Figure 7. A sensitivity analysis is carried out for mixing of HF with moist air, whereby both humidity and initial liquid mass fraction have been varied.

3. Non-equilibrium model (no reactions). This model allows the temperature of the droplet (liquid component) to be different of the temperature of the other compounds in the cloud. The non-equilibrium model determines the phase distribution of the water and the vapour temperature.

A brief assessment of the UDM droplet model has been carried out. In conjunction with the equilibrium thermodynamics model the droplet model is used to set the droplet trajectories and the point of rainout only. In conjunction with the non-equilibrium thermodynamics model, it additionally calculates the droplet mass and the liquid droplet temperature. The initial drop size is taken as the minimum of the droplet size calculated by mechanical break-up and flashing break-up. Further work needs to be carried out to further improve the model for flash calculations and droplet correlations. A limited sensitivity analysis has been carried out in which droplet trajectories etc. have been compared. It is confirmed that for reducing droplet size the non-equilibrium model converges to the equilibrium model.

4. Pool spreading and vaporisation

If the droplet reaches the ground, rainout occurs, i.e. removal of the liquid component from the cloud. This produces a liquid pool which spreads and vaporises (see Figure 8). Vapour is added back into the cloud and allowance is made for this additional vapour flow to vary with time.

Pool spreading/evaporation.

The UDM source term model PVAP calculates the spreading and vapour flow rate from the pool. Different models are adopted depending whether the spill is on land or water, and whether it is an instantaneous or a continuous release. The original version of PVAP was developed by Cook and Woodward[24].

The pool spreads until it reaches a bund or a minimum pool thickness. The pool may either boil or evaporate while simultaneously spreading. For spills on land, the model takes into account heat conduction from the ground, ambient convection form the air, radiation and vapour diffusion. These are usually the main mechanisms for boiling and evaporation. Solution and possible reaction of the liquid in water are also included for spills on water, these being important for some chemicals. These effects are modelled numerically, maintaining mass and heat balances for both boiling and evaporating pools. This allows the pool temperature to vary as heat is either absorbed by the liquid or lost during evaporation.

The PVAP results were compared by David Webber against the SRD/HSE model GASP for a range of scenarios with the aim of testing the various sub-modules. Thus further work for improvement was identified. See the UDM Technical Reference Manual[3] for further details and model validation against experimental data.

Addition of pool vapour back to the cloud.

For a continuous release, the rate of generation of vapour from the spilt liquid is added to the vapour already in the cloud to give a total flow rate for the combined source. When the release stops there may then be a period of vapour generated from the liquid pool alone.

In the case of an instantaneous release the vapour produced by the spilt liquid is added back into the cloud, so long as part of the cloud still covers the point at which the pool was formed by the rained-out liquid. If the

----

spilt liquid all evaporates while covered by the cloud then all that is produced is an instantaneous cloud. If the liquid has not all evaporated then once the upwind edge of the cloud has moved past the pool any remaining liquid is assumed to form a continuous source of vapour.

5. Validation

The above sections described the verification and the validation against *wind-tunnel* experiments for the individual UDM modules. This section is concerned with the validation of the overall model against large-scale *field* experiments.

The basis and choice of these experiments stems from both the model evaluation carried out by Hanna et al.[25] and from the ongoing EEC SMEDIS[26] program (Scientific Model Evaluation of Dense Gas Dispersion Models). Thus seven sets of continous experiments and one set of instantaneous experiments were selected:

1.   Prairie Grass (continuous passive dispersion of sulphur dioxide; 10 experiments).
2.   Desert Tortoise (continuous elevated two-phase ammonia jet; 4 experiments)
3.   FLADIS (continuous elevated two-phase ammonia jet; 3 experiments)
4.   EEC (continuous elevated two-phase propane jet; 2 experiments)
5.   Goldfish (continuous elevated two-phase HF jet; 3 experiments)
6.   Maplin Sands (continuous evaporation of LNG from pool; 4 experiments)
7.   Burro (continuous evaporation of LNG from pool; 2 experiments)
8.   Thorney Island (instantaneous unpressurised ground-level release of Freon-12; 9 experiments)

Each of the above experimental sets were statistically evaluated to determine the accuracy and precision of the UDM predictions with the observed data. Formulas adopted by Hanna et al.[25] were calculated to calculated the geometric mean bias (under or over-prediction of mean) and mean variance (scatter from observed data) for each validation run. This was carried out for centre-line concentrations, cloud widths, and (for the SMEDIS experiments) also off centre-line concentrations.

The overall performance of the UDM in predicting both peak centreline concentration and cloud widths was found to be good for the above experiments.

-       The predictions for the neutrally buoyant Prairie Grass experiments (Figure 9) and the aerosol releases of Desert Tortoise (Figure 10), FLADIS and EEC were found to be very good.
-       Good agreement was also obtained for the Goldfish experiments prior to the passive transition (Figure 11). A more strict passive transition criterion would improve the results in the far field. This conclusion also applied for the Maplin Sand experiments. Good resuls were obtained for Burro.
-       Good agreement was obtained for the instantaneous heavy-gas Thorney Island experiments (Figure 12).

Following an analysis of the experiments, recommendations for future work may centre upon the enhancement of the heavy spread formulation to include a gravity collapse criteria, improved modelling of dispersion from a pool and improved transition to passive dispersion. See the UDM Technical Reference Manual[3] for further details.

6. Conclusions

Each of the modules in the UDM has been investigated and verified in detail in conjunction with a literature review and a sensitivity analysis. The modules have been corrected where necessary, validated where possible, and been compared with similar third-party sofware applications. This has been carried out in extensive detail for the entire basic continuous model [phases of dispersion (passive, jet, heavy), equilibrium thermodynamics without rainout] and to some extent also the instantaneous model [far-field passive dispersion, ground-level heavy-gas dispersion]. Following this work the UDM comparison against large-scale experiments improved considerably, despite the elimination of tuning coefficients.

A detailed assessment and limited corrections have been carried out for the transition to passive, finite-duration releases, HF thermodynamics, and heat/water transfer from the substrate.
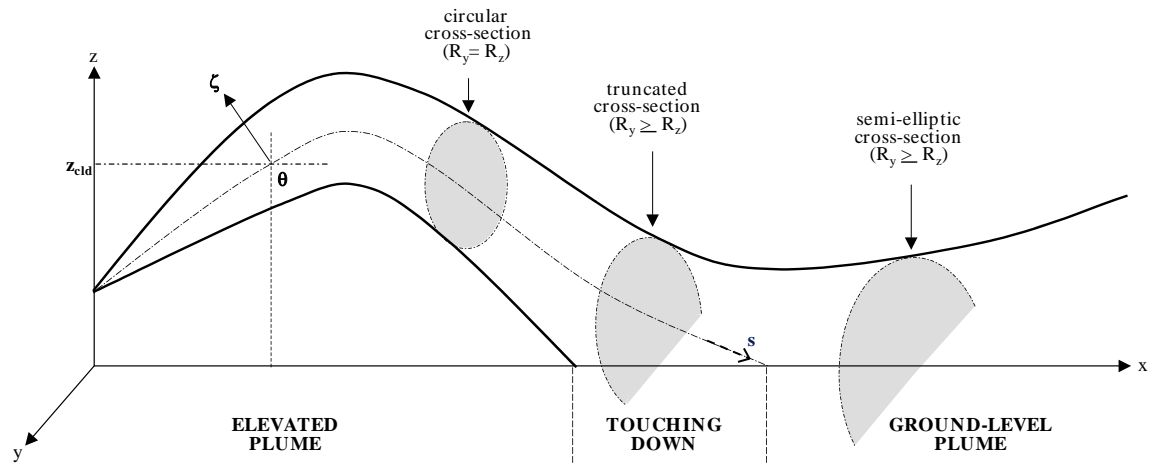
A brief assessment has been carried out for droplet modelling, pool spreading/evaporation, the link between pool and dispersion model, pressurised instantaneous expansion, lift-off and mixing-layer logic, and time-dependent releases. A more detailed assessment is to be carried out for these areas.

The key differences resulting from the modelling changes between the old UDM model (PHAST 5.20) and the new UDM model (PHAST 6.0) are as follows:
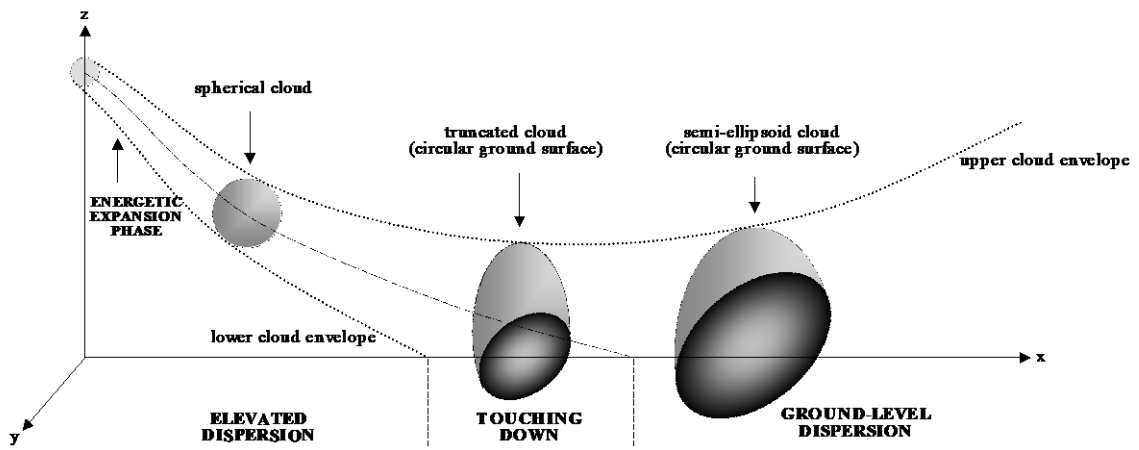
- larger concentrations for far-field passive dispersion [corrections to passive dispersion logic]
- lower concentrations for near-field elevated jet dispersion [increased jet and cross-wind entrainment coefficients, added near-field dispersion]
- larger ground-level heavy-gas spreading (wider clouds) [increased cross-wind spreading parameter]
- often increased water aerosol formation and therefore hotter clouds [new thermodynamics models]

The key advantages of the new UDM model with respect to other typical dispersion models can be summarised as follows:

(a) a single model for the entire dispersion regime from the point of release to the far-field dispersion including possible rainout and pool re-evaporation; this eliminates discontinuities and matching problems

(b) a very extensive verification and validation to ensure that the model shows the correct behaviour and produces accurate predictions

(c) integration within the user-friendly and well-established DNV consequence-modelling package PHAST and the risk-analysis package SAFETI. This enables plotting, linking with discharge/fire/explosion models, toxic/flammable impact and risk calculations.

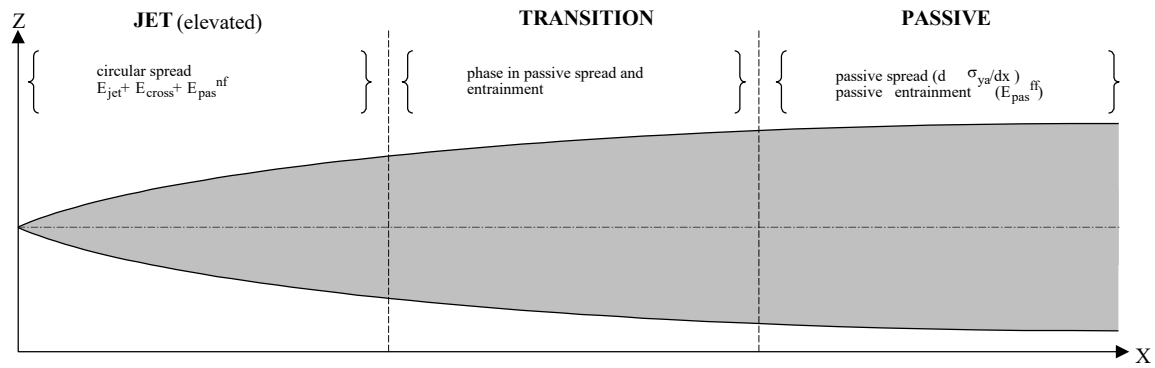(d) rigid procedures and control using ISO9001/TickIT quality standards

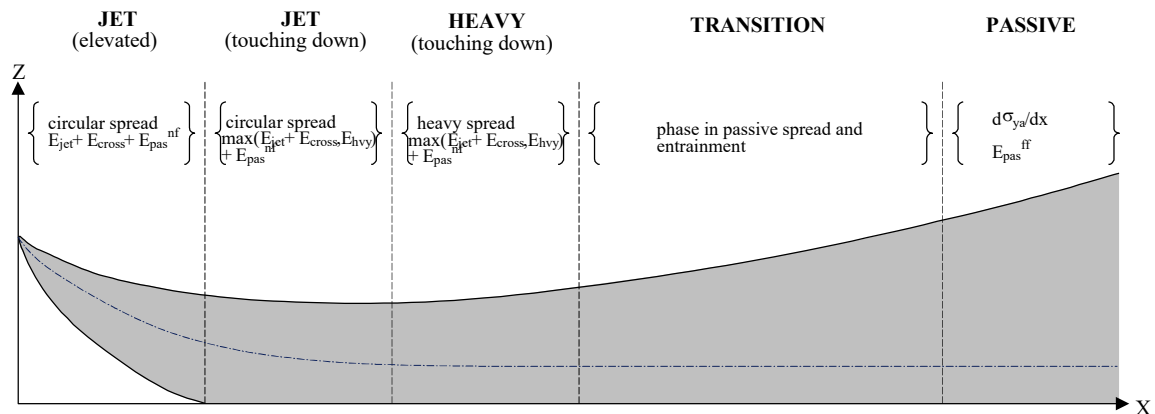--

circular
cross-section
$(R_y = R_z)$

truncated
cross-section
$(R_y \geq R_z)$

semi-elliptic
cross-section
$(R_y \geq R_z)$

z

ζ

z_{cld}

θ

s

x

y

**ELEVATED
PLUME**

**TOUCHING
DOWN**

**GROUND-LEVEL
PLUME**

(a) continuous dispersion

z

spherical cloud

truncated cloud
(circular ground surface)

semi-ellipsoid cloud
(circular ground surface)

upper cloud envelope

**ENERGETIC
EXPANSION
PHASE**

lower cloud envelope

x

y

**ELEVATED
DISPERSION**

**TOUCHING
DOWN**

**GROUND-LEVEL
DISPERSION**

(b) instantaneous dispersion

Figure 1.   UDM cloud geometry

Z

JET (elevated)   **TRANSITION**   **PASSIVE**

circular spread
$E_{jet} + E_{cross} + E_{pas}^{nf}$

phase in passive spread and entrainment

passive spread (d σ_{ya}/dx)
passive entrainment (E_{pas}^{ff})

X

(a) elevated jet/plume (no touching down)

Z

JET (elevated) | **JET** (touching down) | **HEAVY** (touching down) | **TRANSITION** | **PASSIVE**

circular spread
$E_{jet} + E_{cross} + E_{pas}^{nf}$

circular spread
$\max(E_{jet} + E_{cross}, E_{hvy}) + E_{pas}^{nf}$

heavy spread
$\max(E_{jet} + E_{cross}, E_{hvy}) + E_{pas}^{nf}$

phase in passive spread and entrainment

$d\sigma_{ya}/dx$

E_{pas}^{ff}

X

(b) jet/plume becomes passive during touching down

Z

JET (elevated) | **JET** (touching down) | **JET** (ground level) | **HEAVY** (ground level) | **TRANSITION** | **PASSIVE**

circular spread
$E_{jet} + E_{cross} + E_{pas}^{nf}$

circular spread
$\max(E_{jet} + E_{cross}, E_{hvy}) + E_{pas}^{nf}$

circular spread
$\max(E_{jet}, E_{hvy})$

heavy spread
E_{hvy}

phase in passive spread and entrainment

$d\sigma_{ya}/dx$

E_{pas}^{ff}

X
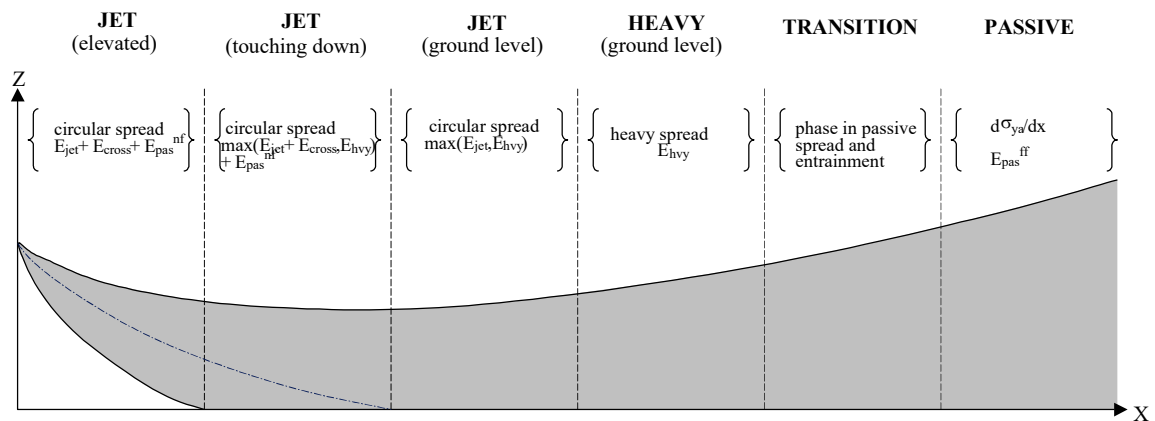
(c) jet/plume become passive after touch down

Figure 2.   Phases in UDM cloud dispersion for range of scenarios

The figures indicate for each phase the type of spreading (circular jet, heavy or passive) and the mechanism of entrainment (E_{jet} = jet; E_{cross} = cross-wind; E_{pas}^{ff} = near-field elevated passive, E_{hvy} = ground-level heavy, E_{pas}^{ff} = far-field passive). Along the transition zone the near-field spread/entrainment are phased out and the far-field spread/entrainment are phased in.
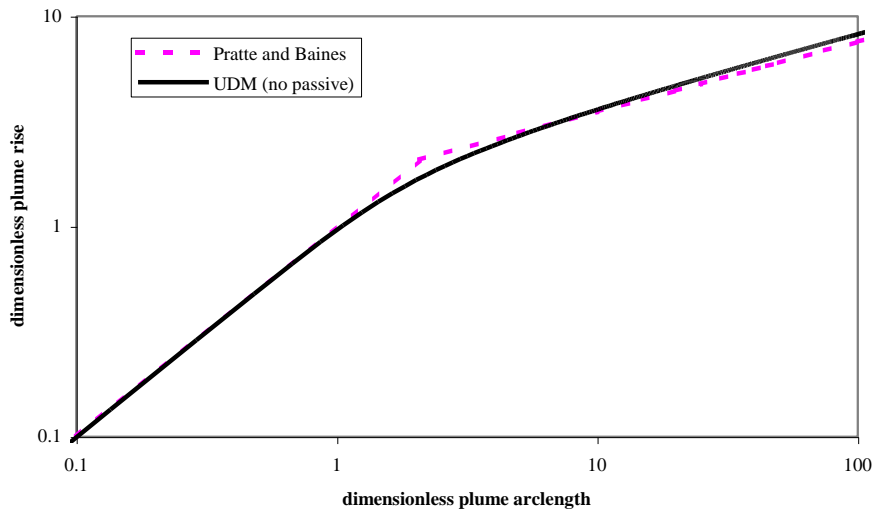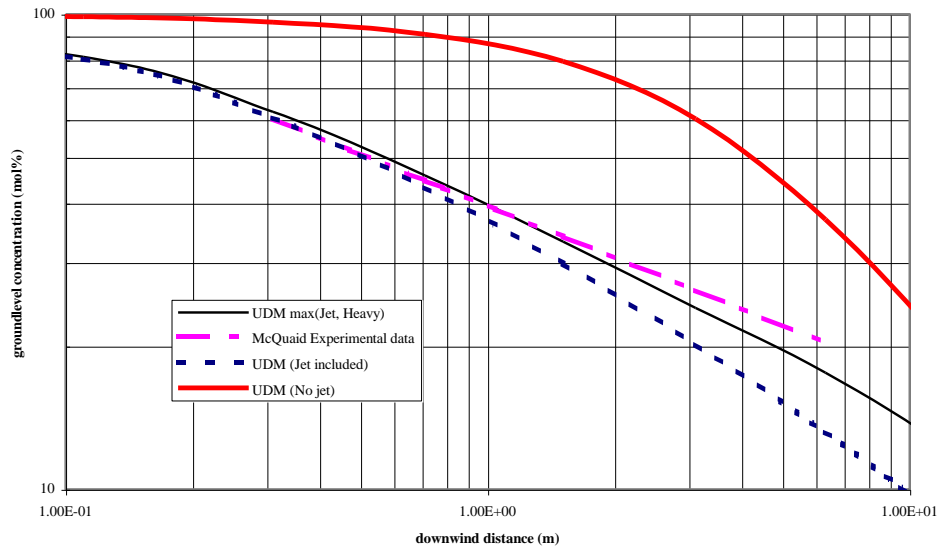

(a)   case of no ambient turbulence; comparison against Pratte and Baines
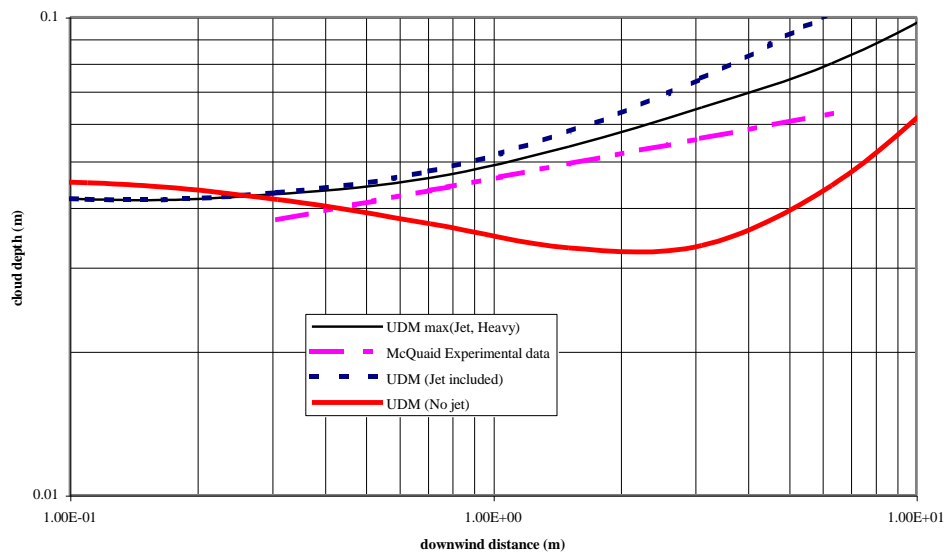   correction (jet/ambient velocity ratio = 13)
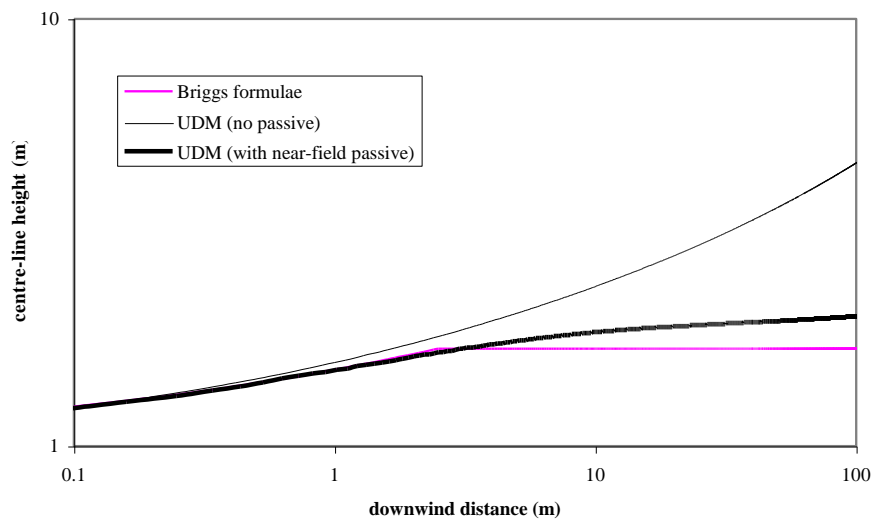
(b)   case of ambient turbulence; comparison against Briggs plume rise formula
        (jet/ambient velocity ratio = 4.6)

**Figure 3.   Comparison of UDM results against plume-rise correlations for
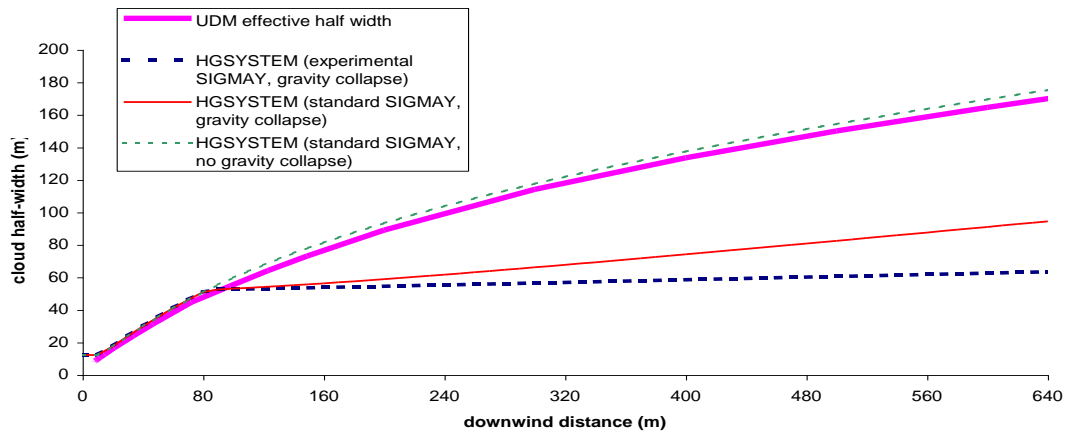   vertical neutrally buoyant jet**

(a) ground-level concentration c_{ov} (mole %)

(b) height $H_{1/2}$ (m) at which concentration is halved

Figure 4.   McQuaid experiment 3; experimental data and UDM predictions assuming (i) $E_{tot} = E_{hvy}$, (ii) $E_{tot} = E_{hvy}+E_{jet}$, (iii) $E_{tot} = max(E_{hvy},E_{jet})$

(a) effective cloud half-width W_{eff}
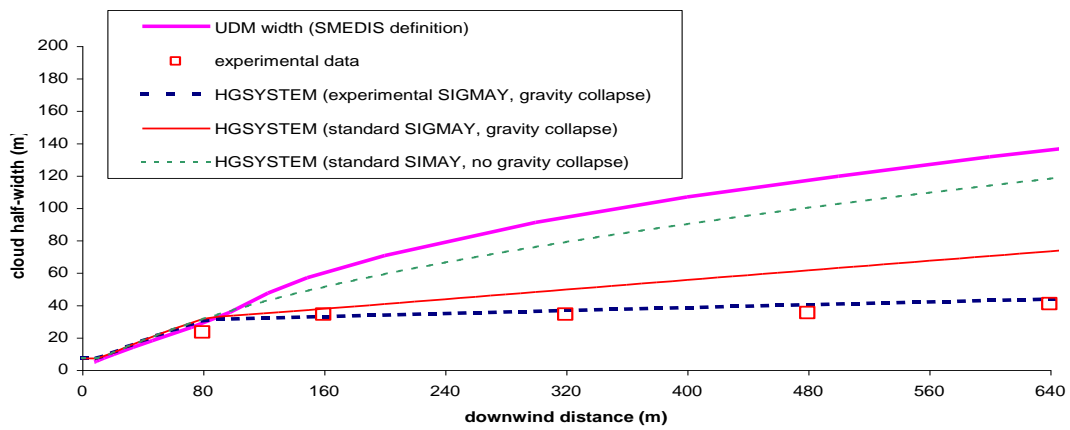
(b) cloud half-width (SMEDIS definition)
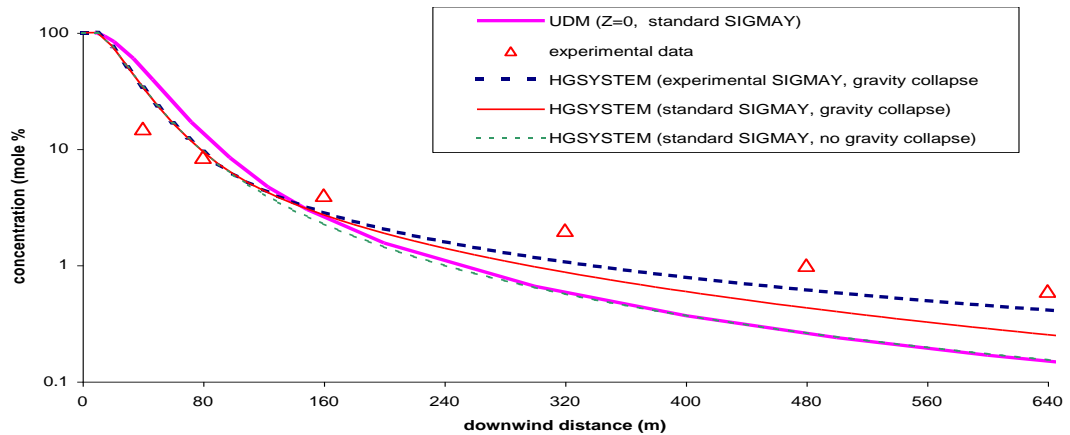
(c) centre-line ground-level concentration

Figure 5.   **HTAG experiment 140; experimental data and UDM/HEGADAS predictions: (i) UDM [use HEGADAS wind-speed profile and value for n], (ii) HEGADAS (standard σ_{ya} , no gravity collapse), (iii) HEGADAS (standard σ_{ya} , gravity collapse), (iv) HEGADAS (experimental σ_{ya} , gravity collapse)**
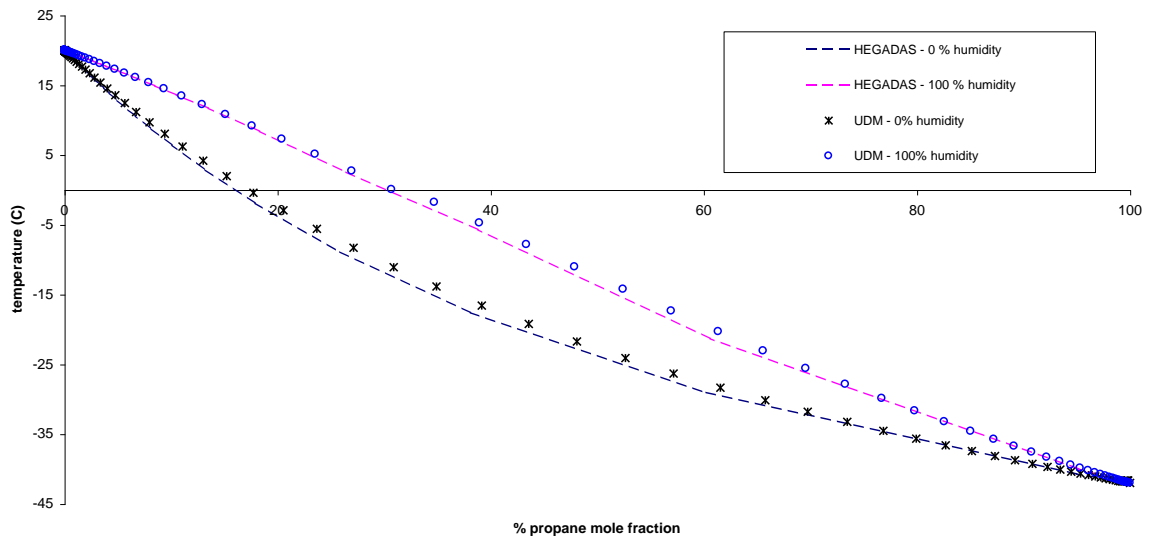
(a) mixing of propane vapour (-42C) with air (20C)
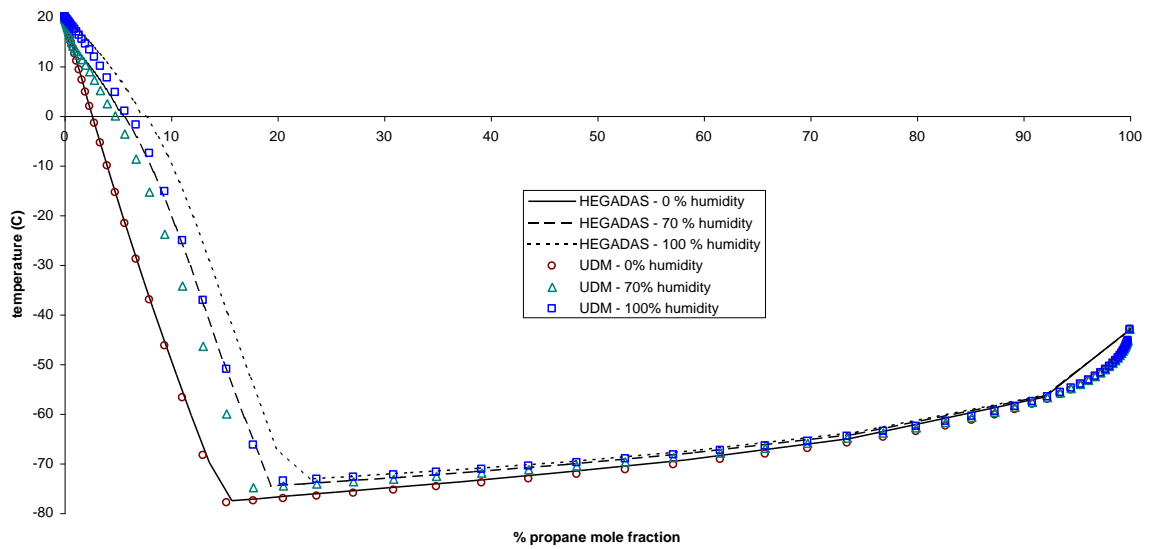
(b) mixing of propane liquid (-43C) with air (20C)

Figure 6. **Temperature predictions by HEGADAS and UDM thermodynamics equilibrium models for mixing of propane (vapour or liquid) with air (dry or humid)**
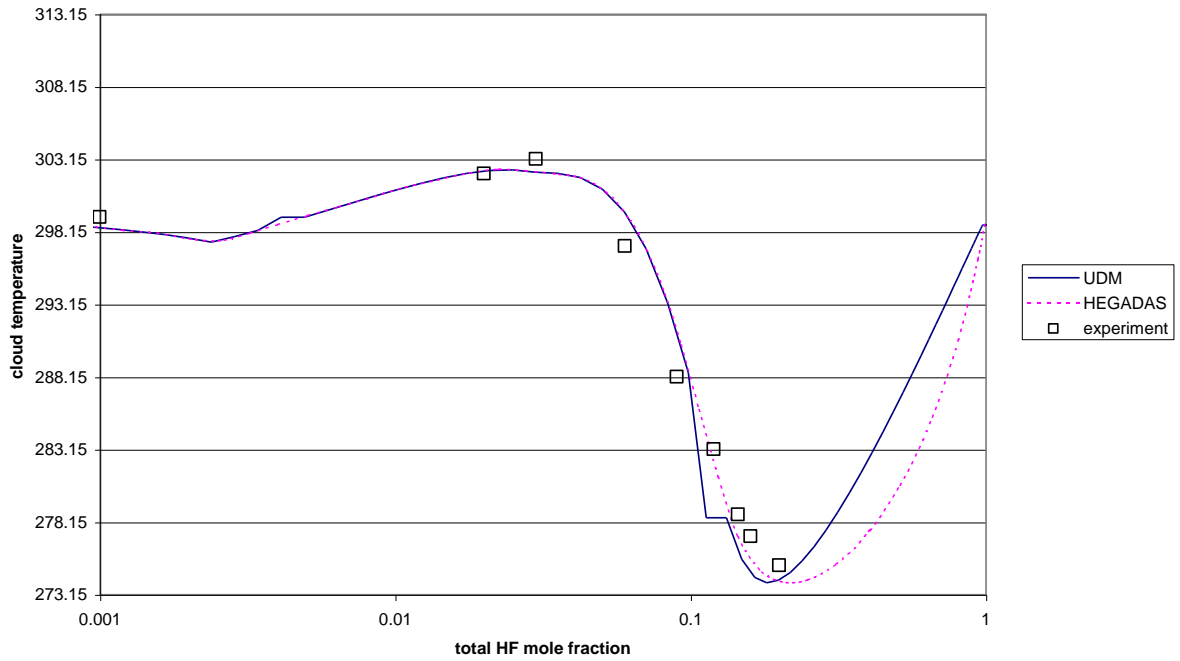

Figure 7. **Mixing at 26C of HF vapour with moist air (humidity = 50%); HEGADAS and UDM thermodynamic test-bed predictions**

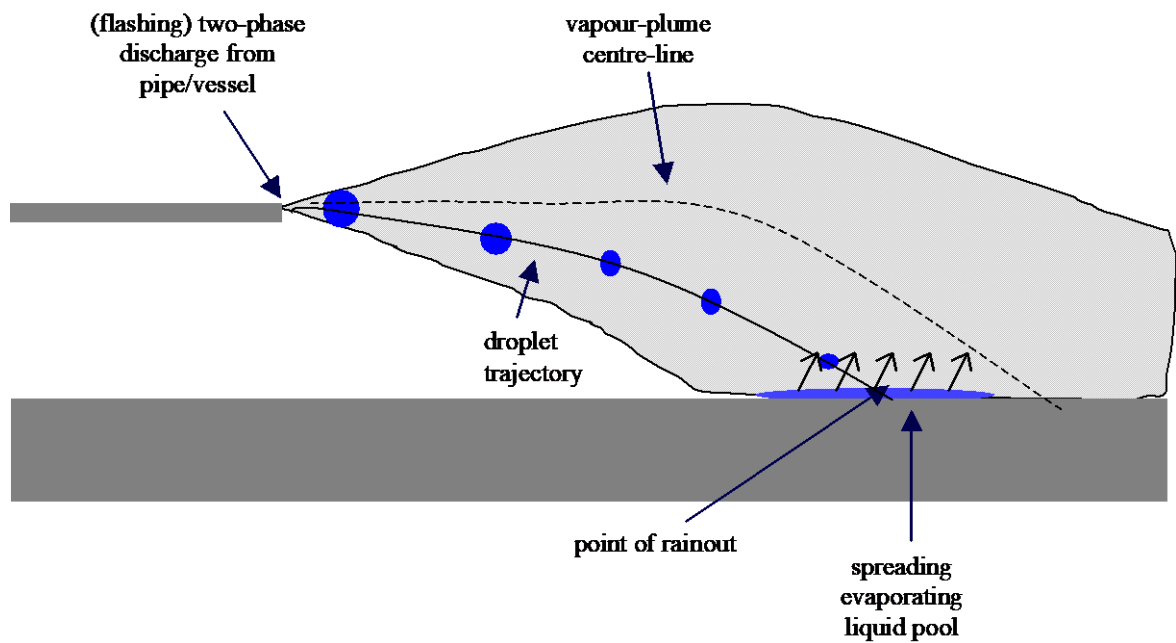**Figure 8.** **Droplet evaporation, rainout, and pool spreading/evaporation.**

Prairie Grass 8 - Elevated release of Sulfur Dioxide

(a) mol % concentration

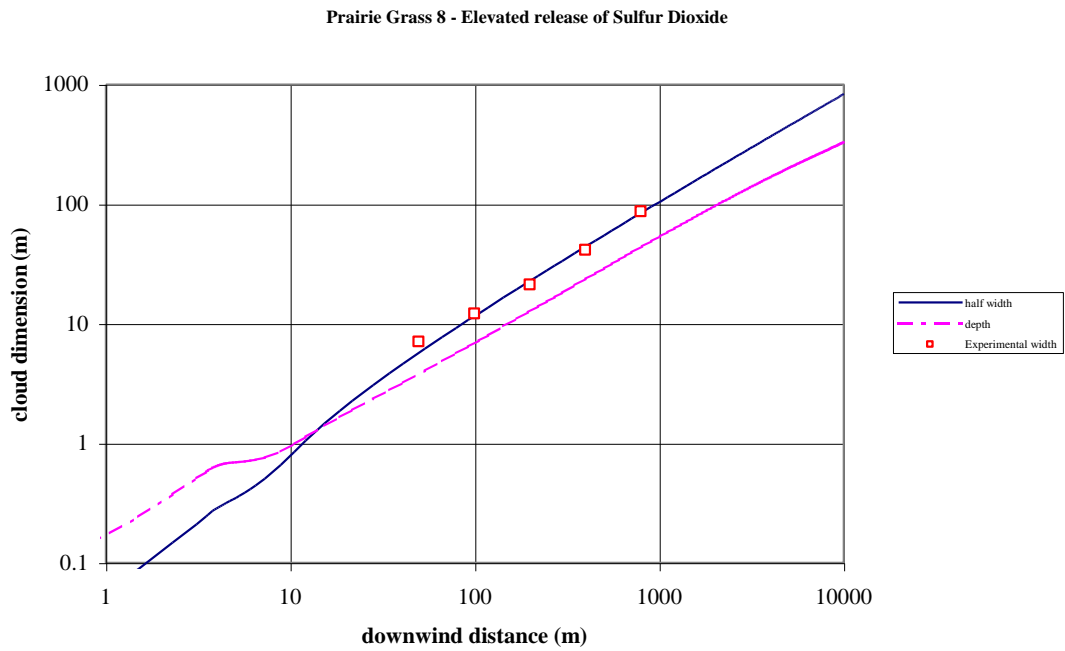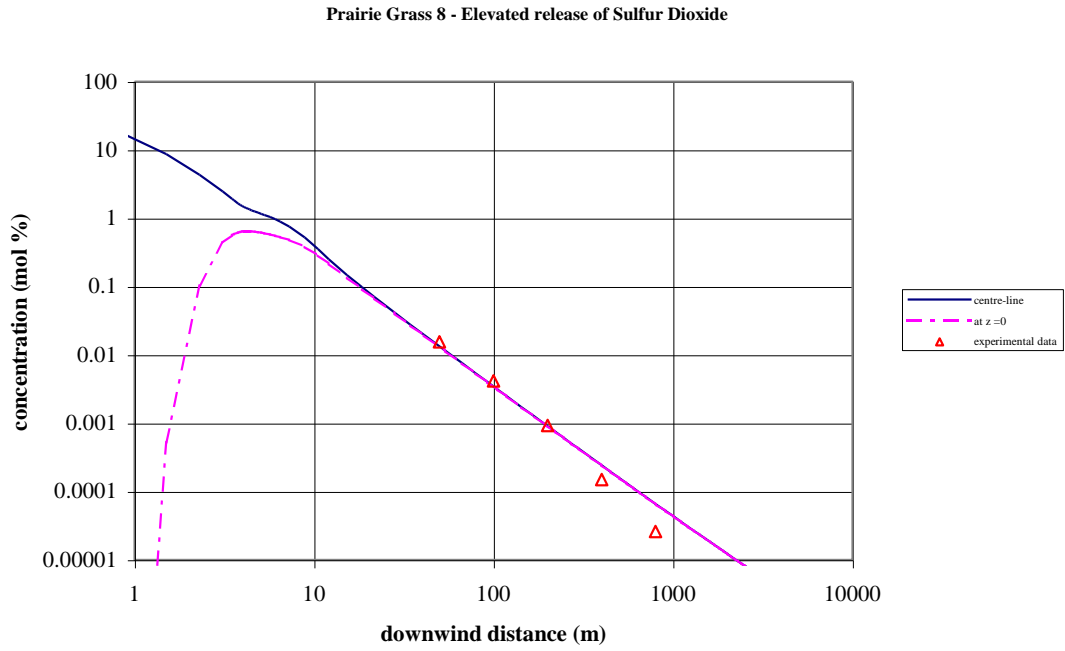**Prairie Grass 8 - Elevated release of Sulfur Dioxide**

(b) cloud dimensions

Figure 9. UDM validation against Prairie Grass experiment 8 (passive dispersion)

Desert Tortoise 2 - Ammonia Aerosol

(a) mol % concentration

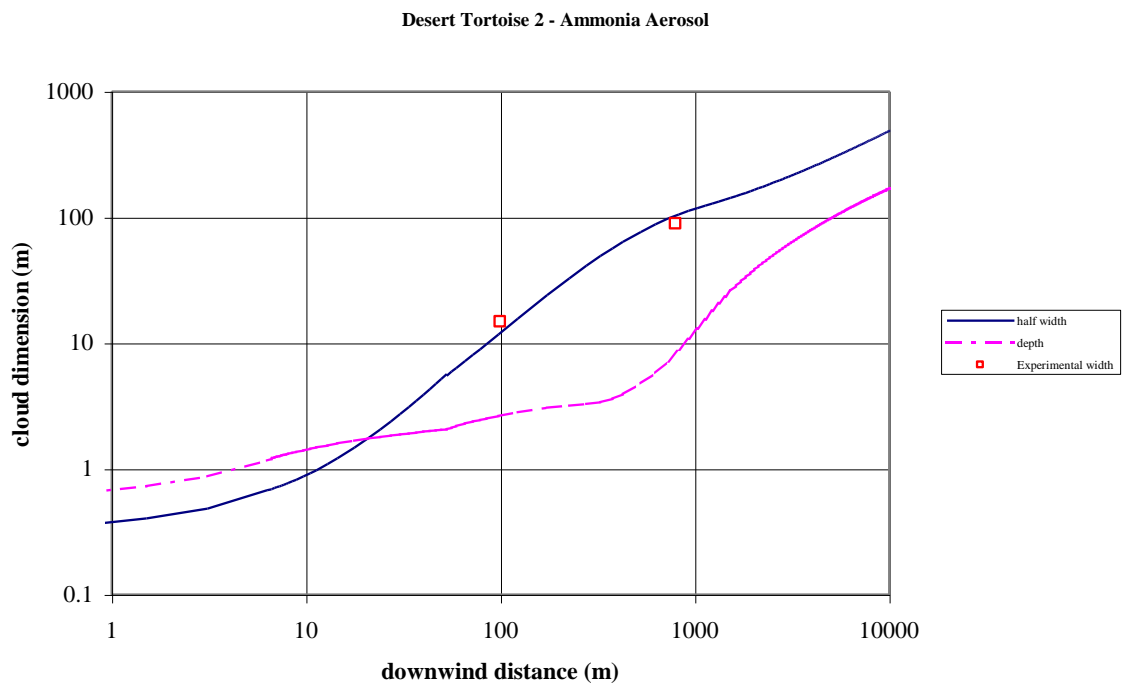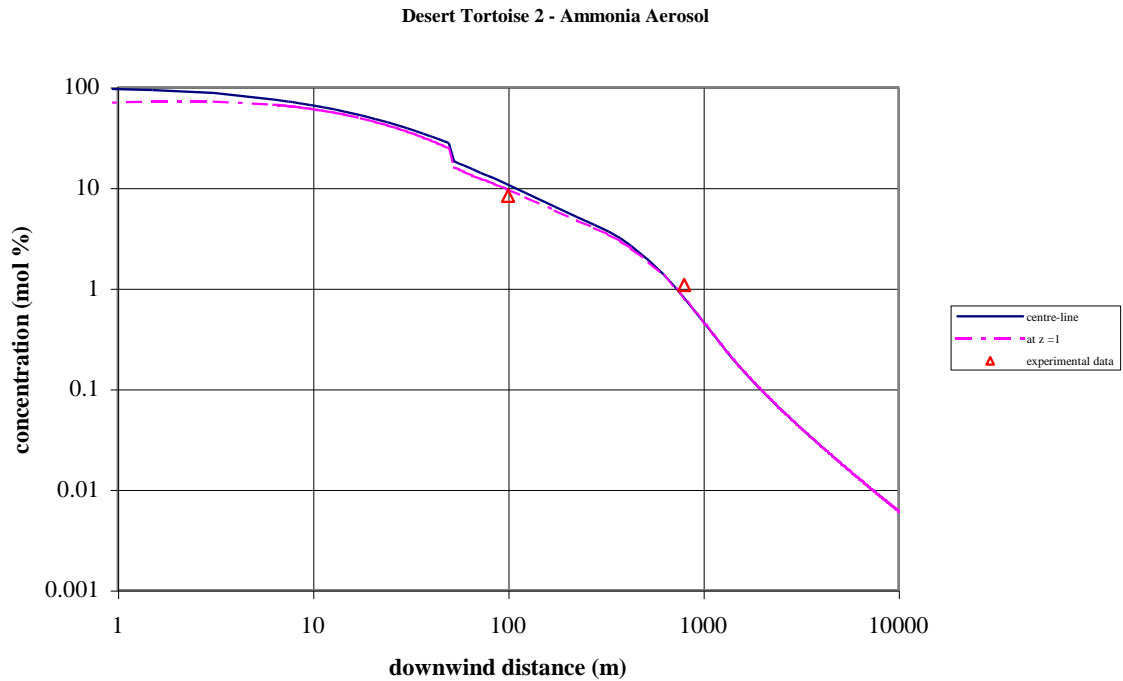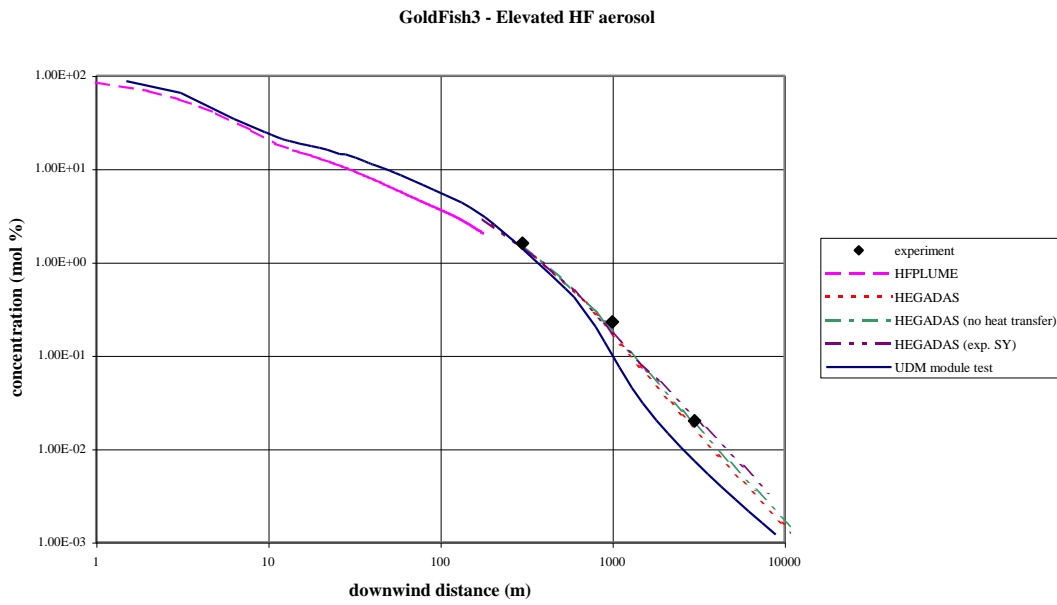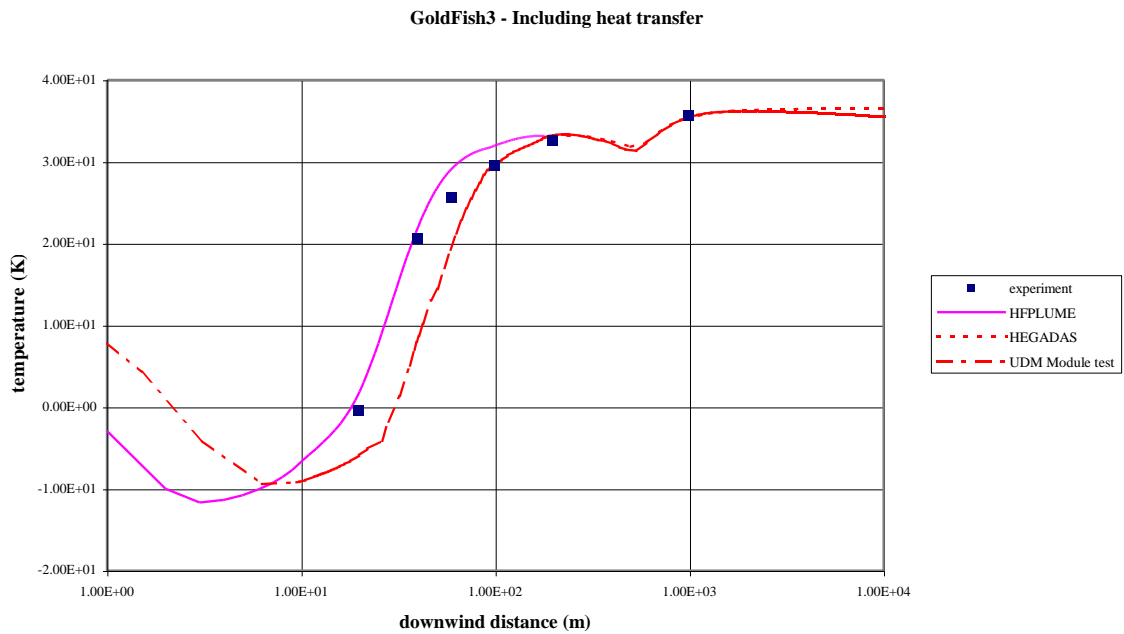**Desert Tortoise 2 - Ammonia Aerosol**

(b) cloud dimensions

Figure 10. UDM validation against Desert Tortoise 2 (two-phase ammonia jet)

GoldFish3 - Elevated HF aerosol

(a) maximum concentration versus downwind distance

GoldFish3 - Including heat transfer

(b) temperature versus downwind distance

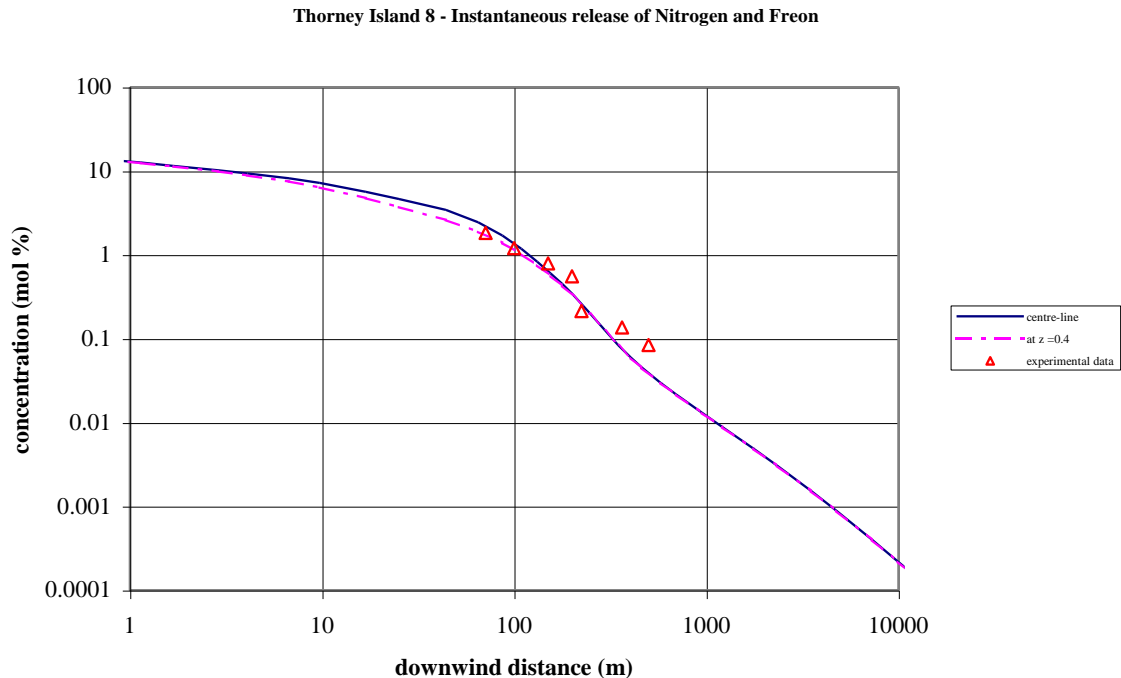**Figure 11.   Goldfish 3 simulations for HFPLUME/HEGADAS (including heat transfer) and UDM**

Thorney Island 8 - Instantaneous release of Nitrogen and Freon

Figure 12.   UDM validation against Thorney Island 8 (instantaneous heavy-gas dispersion)

Nomenclature

A_{cld}	cross sectional area of continuous cloud, m^2
A_{side}	effective side area of instantaneous plume, m^2
A_{top}	effective top area of instantaneous plume, m^2
c	concentration, kg of component $/m^3$
c_o	centre-line concentration, kg of component $/ m^3$
E_{cross}	cross-wind entrainment rate, kg/s or kg/m/s
E_{hvy}	dense gas entrainment rate, kg/s or kg/m/s
E_{jet}	jet (high-momentum) entrainment rate, kg/s or kg/m/s
E_{pas}^{nf}	near-field passive dispersion entrainment rate, kg/s or kg/m/s
E_{pas}^{ff}	far-field passive dispersion entrainment rate, kg/s or kg/m/s
E_{tot}	total dispersion entrainment rate, kg/s or kg/m/s
F_{drag}^{air}	airborne drag force, N/m or N
F_{drag}^{ground}	ground drag force, N/m or N
$F_h(x)$	horizontal distribution function for concentration (-)
$F_v(\zeta)$	vertical distribution function for concentration (-)
H_{eff}	effective height of cloud after full touchdown, m [height prior to full touchdown = $H_{eff}(1+h_d)$]
h_d	fraction of bottom half of cloud which is above the ground [h_d=0,1 for grounded,elevated cloud]
I_{x2}	horizontal plume momentum in excess to ambient momentum [$I_{x2}= I_x - m_{cld}u_a$], kg m/s or kg/m/s^2
I_z	vertical component of plume momentum, kg m/s or kg/m/s^2
m	exponent of horizontal distribution function for concentration (-)
m_{cld}	mass in plume (instantaneous release, kg) or mass rate in plume (continuous release, kg/s)
m_{wv}^{gnd}	water-vapour added from the substrate, kg or kg/s
n	exponent of vertical distribution function for concentration (-)
P_{above}	perimeter length of jet, m
$P_v^w(T)$	saturated vapour pressure as function of temperature T (K) for water, Pa

----

q_{gnd}	heat transfer rate from ground to cloud, J or J/s
R_y	term in cross-wind concentration profile, m $[R_y = R_y(x) = 2^{1/2}\sigma_y(x)]$
R_z	term in vertical concentration profile, m $[R_z = R_z(x) \, 2^{1/2}\sigma_z(x)]$
Ri_*	layer Richardson number, (-)
s	arclength along centre-line of the plume, m
S_{gnd}	footprint area for instantaneous plume, m^2
t	time since onset of release, s
T_a	ambient temperature, K
T_{gnd}	substrate temperature, K
T_{vap}	temperature of vapour phase of the cloud, K
u_*	friction velocity for cloud, m/s
u_a	ambient wind-speed, $u_a = u_a(z)$, m/s
u_{cld}	total cloud speed, m/s
u_{ref}	value of ambient windspeed u_a at reference height $z = z_{ref}$, m/s
u_{side}	entrainment velocity through sides of plume, m/s
u_{top}	entrainment velocity through top of plume, m/s
u_x, u_z	horiontal and vertial component of cloud speed u_{cld}, m/s
V_{cld}	volume of cloud, m^3
W_{eff}	effective half width of plume, m
W_{gnd}	footprint half-width for continuous plume, m
x	horizontal downwind distance, m
x_{cld}	horizontal downwind position of cloud, m
y	crosswind distance, m
z	vertical height, m
z_{cld}	cloud centre-line height above ground, m
z_o	surface roughness length, m
z_c	height above ground of cloud centroid, m
z_{ref}	reference height, m

Greek letters

α_1, α_2	jet- and cross-wind entrainment coeficient , (-)
γ	side-entrainment coefficient for instantaneous heavy-gas dispersion, (-)
Γ	Gamma function (-)
θ	angle to horizontal of plume, rad; $\theta = 0$ corresponds to a horizontal plume (in downwind x-direction), while $\theta = \pi/2$ corresponds to a vertical upwards plume (in z-direction)
ζ	distance perpendical to plume centre-line, m
κ	Von Karman constant, $\kappa = 0.4$ (-)
ρ_{cld}	density of plume, kg/m^3
ρ_a	density of ambient air, kg/m^3
σ_{ya}	standard empirical correlation for passive crosswind dispersion coefficient, m
σ_{za}	standard empirical correlation for vertical crosswind dispersion coefficient, m

Acknowledgements

References

[1] Woodward, J.L, Cook, J., and Papadourakis, A., "Modelling and validation of a dispersing aerosol jet", Journal of hazardous materials 44, pp. 185-207 (1995)

[2] Woodward, J.L, and Papadourakis, A., "Reassessment and reevaluation of rainout and drop size correlation for an aerosol jet", Journal of hazardous materials 44, pp. 209-230 (1995)

[3] Witlox, H.W.M., and Holt, A., "Unified Dispersion Model – Technical Reference Manual", UDM Version 6.0, June 1999, Det Norske Veritas, London (1999)

---

[4] Webber, D.M., S.J. Jones, G.A. Tickle and T. Wren, "A model of a dispersing dense gas cloud and the computer implementation D*R*I*F*T. I: Near instantaneous release." SRD Report SRD/HSE R586 April 1992, and ". . . II: Steady continuous releases." SRD Report SRD/HSE R587 April 1992

[5] Morton, B.R., Taylor, G.I., and Turner, J.S.,"Turbulent gravitational convection from maintained and instantaneous sources", Proc. R.Soc., Series A, 234, 1 (1956)

[6] Ricou, F.P. and Spalding, D.B., "Measurements of entrainment by aximsymmetrical turbulent jets", J. Fluid Mech. 11 (1), pp. 21-31 (1961)

[7] Briggs, G.A., "Plume rise and buoyancy effects", Ch. 8 (pp. 327-366) in Randerson, D. (ed.), "Atmospheric Science and Power Production", Technical Information Center, US Department of Energy, Report DOE/TIC-27601 (1984)

[8] Disselhorst, J.H.M., "The incorporation of atmospheric turbulence in the KSLA Plumepath program", Shell Internationale Research Maatschappij B.V., The Hague, AMGR.84.059 (1984)

[9] Havens, J., and Spicer, T.O.,"Development of an atmospheric dispersion model for heavier-than-air mixtures" (DEGADIS model), Vols. 1- 3, University of Arkansas (1985)

[10] Britter, R.E., "A review of mixing experiments relevant to dense gas dispersion", IMA Conference on stably stratified flow and dense gase dispersion ", April 1986, Chester, Oxford University Press (1988)

[11] McFarlane, K., "Development of plume and jet release models", International Conference and workshop on modelling and mitigating the accidental releases of hazardous materials, AIChE, CCPS, New Orleans, LA, May 20-24, pp. 657-688 (1991)

[12] McAdams, W.H., "Heat Transmission", McGraw-Hill (1954)

[13] Holman, J.I., "Heat transfer", 5th Ed., McGrawHill (1981)

[14] Witlox, H.W.M., "Technical description of the heavy-gas-dispersion program HEGADAS", Report TNER.93.032, Thornton Research Centre, Shell Research, Chester, England (1993)

[15] Van Ulden, A.P., "A new bulk model for dense gas dispersion: two-dimensional spread in still air, in "Atmospheric dispersion of heavy gases and small particles" (Ooms, G. and Tennekes, H., eds.), pp. 419-440, Springer-Verlag, Berlin (1984)

[16] Pratte, B.D., and Baines, W.D., "Profiles for the round turbulent jet in a cross flow", Proc. ASCE, HY (Journal of the Hydraulics Division), Vol. 6, pp. 53-64 (1967)

[17] McQuaid, J., "Some experiments on the structure of stably stratified shear flows", Technical Paper P21, Safety in Mines Research Establishment, Sheffield, UK (1976)

[18] Petersen, R.L., and Ratcliff, M.A., "Effect of homogeneous and heterogeneous surface roughness on HTAG dispersion", CPP Incorporated, Colorado. Contract for API, Draft Report CPP-87-0417 (1988)

[19] Witlox, H.W.M., McFarlane, K., Rees, F.J., and Puttock, J.S., "Development and validation of atmospheric dispersion models for ideal gases and hydrogen fluoride", Part II: HGSYSTEM program user's manual, Report RKER.90.016, Thornton Research Centre, Shell Research, Chester, England (1990)

[20] Ermak, D.L., "Unpublished notes on downwind spreading formulation in finite-duration release version of SLAB", Lawrence Livermore National Laboratorym, California (1986)

[21] Witlox, H.W.M, Two-phase thermodynamics model for mixing of a non-reactive multi-compound pollutant with moist air, Report TNER.93.022, Thornton Research Centre, Shell Research, Chester, England (1993)

[22] Witlox, H.W.M., "Thermodynamics model for mixing of moist air with pollutant consisting of HF, ideal gas and water", Report TNER.93.021, Thornton Research Centre, Shell Research, Chester, England (1993)

[23] Schotte, W., "Fog formation of hydrogen fluoride in air", Ind. Eng. Chem. Res. 26, pp. 300-306 (1987); see also Schotte, W., "Thermodynamic model for HF formation", Letter from Schotte to Soczek, E.I. Du Pont de Nemours & Company, Du Pont Experimental Station, Engineering Department, Wilmington, Delawere 19898, 31 August 1988

[24] Cook, J. and Woodward, J.L., "A new integrated model for pool spreading, evaporation and solution on land and water", International Conference and Exhibition on Safety, Health and loss prevention in the Oil, Chemical and Process Industries, Singapore, February 15-19 (1993)

[25] Hanna, S.R., D.G.Strimaitis, and J.C.Chang, "Hazard response modelling uncertainty (A quantitative method)", Sigma Research Corp. report, Westford, MA for the API (1991)

[26] Daish, N.C., Britter, R.E., Linden, P.F., Jagger. S.F., and Carissimo, B., "SMEDIS: Scientific Model Evaluation techniques applied to dense gas dispersion models in complex situations", International Conference and Workshop on Modelling the Consequences of Accidental Releases of Hazardous Materials, CCPS, San Francisco, California, September 28 – October 1 (1999)